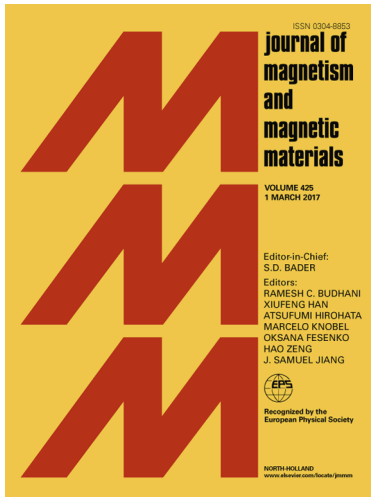

Structural and physical property study of sol – gel synthesized $CoFe_{2-x}Ho_xO_4$ nano ferrites

K.K. Patankar, D.M. Ghone, V.L. Mathe, S.D. Kaushik

PII: S0304-8853(17)33587-4
DOI: https://doi.org/10.1016/j.jmmm.2018.01.039
Reference: MAGMA 63617

To appear in: *Journal of Magnetism and Magnetic Materials*

Received Date: 14 November 2017
Revised Date: 8 January 2018
Accepted Date: 15 January 2018

Please cite this article as: K.K. Patankar, D.M. Ghone, V.L. Mathe, S.D. Kaushik, Structural and physical property study of sol – gel synthesized $CoFe_{2-x}Ho_xO_4$ nano ferrites, *Journal of Magnetism and Magnetic Materials* (2018), doi: https://doi.org/10.1016/j.jmmm.2018.01.039

Structural and physical property study of sol – gel synthesized $CoFe_{2-x}Ho_xO_4$ nano ferrites

K. K. Patankar[1#], D. M. Ghone[1],V. L. Mathe[2] and S. D. Kaushik[3*]

[1]Department of Physics, Rajaram College, Kolhapur-416004

[2]Department of Physics, SavitribaiPhule University, Pune-411007

[3]UGC-DAE-Consortium for Scientific Research, Mumbai Centre, R-5 Shade, BARC, Mumbai-400085

Corresponding author email id: [#]ketakiketan@gmail.com and [*]sdkaushik@csr.res.in

Abstract:

$CoFe_{2-x}Ho_xO_4$ (x=0.00, 0.05, 0.10, 0.15, 0.20) ferrites were prepared by the suitably modified Sol-Gel technique. X-ray diffraction (XRD) analysis revealed that the substituted samples show phase pure formation till 10% substitution, which is far higher phase pure than the earlier reports. Upon further substitution an inevitable secondary phase of $HoFeO_3$ along with the spinel phase despite regulating synthesis parameters in the sol-gel reaction route. These results are further corroborated more convincingly by room temperature neutron diffraction. Morphological features of the ferrites were studied by Scanning Electron Microscopy (SEM). The magnetic parameters viz. the saturation magnetization(Ms), coercivity(Hc) and remanence(Mr) were determined from room temperature isothermal magnetization. These parameters were found to decrease with increase in Ho substitution. The decrease in magnetization is analyzed in the light of exchange interactions between rare earth and transition metal ions. Magnetostriction measurements revealed interesting results and the presence of a secondary phase was found to be responsible for decreased measured magnetostriction values. The solubility limit of Ho in $CoFe_2O_4$ lattice is also reflected from the X-ray and neutron diffraction analysis and magnetostriction studies.

Introduction:

Conventional Spinel Ferrites have a plethora of applications in the numerous fields of technology owing to versatility in magnetic and electrical properties [1-2].Research in nano-ferrites is now emerging out as popular area of study due to its diverse applications in food, medicine, electrical and electronics industries [1-2]. Nano-ferrites have revolutionized electronic industry because of intensealterations seen in the investigated properties[3-5]. The properties of the ferrites are influenced by the type of substituent in its basic generic compound namely magnetite (FeO, Fe_2O_3). Electromagnetic properties get markedly alteredby varying the chemical route of synthesis [6-8]. Many researchers have studied rare earth substituted ferrites and have even observed variations in magnetic as well as electrical properties [9-12]. Among ferrites cobalt ferrite ($CoFe_2O_4$) is one of the extensively studied ferrite, it is a hard magnet and has high magnetocrystalline anisotropy constant. The usefulness of $CoFe_2O_4$ ferrite based materials has already been well established in various devices and applications such as magnetostrictive sensors, actuators, super capacitors, drug delivery etc. [13] in $CoFe_2O_4$,which crystallizes in spinel form is promising materials in nano-ferrites form and has been studied for magneto-optical devices and are preferred in high frequency magnetic storage devices. In-fact, the properties of the ferrites can be tailored for a specific application by proper substitution of rare earths in place of ferric ions[14-15]. The purpose to rare earth doping is to enhance the properties like saturation magnetization, permittivity, permeability etc. Present research work communicates the studies on structural, magnetic properties and magnetostriction study of Ho doped Co ferrite. The samples in the present study were prepared by using sol-gel process, in order to get the optimum phase purity the synthesis process was modified appropriately. Post doping studies show that doping Ho in $CoFe_2O_4$ enhances its suitability for application in magneto-mechanical transducers.

Experimental:

The $CoFe_{2-x}Ho_xO_4$(x=0.0, 0.05, 0.10, 0.15, 0.20) were prepared by Sol-gel synthesis technique. The stoichiometric amounts of Cobalt nitrate ($CoNO_3$> 99.9% pure), Holmium nitrate ($HoNO_3$>99.9% pure), Ferric nitrate ($FeNO_3$>99.9% pure) and citric acid (CH_3COOH) were dissolved in distilled water. Auto-combustion of gel takes place and thereafter doped ferrite is formed. Fig 1 depicts the chemical reaction and the reaction mechanism of the rare earth doped

ferrites sample preparation. Pre-sintering was done at 500^0C for 5 hours in furnace. The pellets were then finally sintered at 1000^0C for 10 hours. The procedure for preparation was modified in comparison to that reported earlier [16,17]. Modification was done by altering the oxide to fuel ratio, the pH value and also by varying method as well as time and temperature of sintering. The balance reaction supporting the various compositions of ferrites is given below.

$$CoNO_3+(2-x)FeNO_3 + xHoNO_3 + C_6H_8O_7 + 5H_2O + 2O_2\uparrow \rightarrow CoFe_{2-x}Ho_xO_4 + 3/2N_2\uparrow + 9H_2O\uparrow + 6CO_2\uparrow$$

The phase of sintered materials was confirmed by X-ray diffraction (XRD) using X-ray diffractometer (Bruker D8 advance).For microscopic analysis of the crystal structure, the room temperature neutron diffraction (ND) study was carried out by employing Focusing Crystal Diffractometer (FCD) of UGC-DAECSR Mumbai Center at National Facility for Neutron Beam Research (NFNBR), Dhruva, BARC, Mumbai(India) using the neutrons of wavelength of 1.48 Å[18].The powder samples were filled in the vanadium can, the can was then directly exposed to neutron beam for room temperature ND study. The Neutron diffraction patterns were analyzed for crystal as well as magnetic structure by employing theFULLPROF suit package using Rietveld method [19]. Density measurements were also carried out by liquid immersion technique. Morphological features of Holmium doped cobalt ferrites were studied by Scanning Electron Microscopy (SEM) (JEOL JSM 6360 A). Finally, room temperature magnetization was studied by employing Vibrating Sample Magnetometry (VSM) (LAKESHORE 7307) to explore the magnetic properties. The magnetic properties such as the saturation magnetization (Ms), coercivity (Hc) and remaneance (Mr) were obtained from the hysteresis loops. Magnetostriction measurements were carried out using P3 strain indicator. The strain gauge having 350Ω resistance was fixed on flat polished surface of pellet by using glue. The magnetic field was applied in the direction parallel to the sample plane and length of strain gauge, the magnetostriction was noted as λ. The magnetic field was applied with the help of electromagnet in the range of 0 to 7000 G.

Results and Discussion:

Structural analysis:

The crystal structure of sintered materials was confirmed by X-ray Diffraction (XRD) technique using X-ray diffractometer. Fig2 shows the Rietveld fitted XRD patterns using

Fullprof suite of all the $CoFe_{2-x}Ho_xO_4$(x=0.0, 0.05, 0.10, 0.15 and 0.20) ferrites. The crystal was found to be fitted in the *Fd-3m* cubic space group. For x=0.0, 0.05 and 0.10 samples show single phase spinel ferrite, small amount of secondary phase of $HoFeO_3$ was observed in substituted samples with higher doping concentration ($x \geq 0.10$), which is denoted by asterisk mark (*) in fig 2.A secondary phase became more intense as Ho content was increased. The secondary phase of $HoFeO_3$ is very common and has appeared significantly upon enhancing the doping concentration beyond 4% [20]. Similar result is observed in Er doped Co ferrite for doping concentrations even less than 4% [19]. The limitation in substitution of Holmium is governed due to higher ionic radii of Holmium (104.1 pm) as compared to Iron (69 pm). Though we have modified our sol-gel sample preparation techniques in terms of various options such as levels of pH value of the constituent solutions, changing the sintering temperature and time, thus we could able to get the phase pure sample up to x = 0.10 concentration, and significantly reduce the secondary phase ($HoFeO_3$) for x = 0.15 and 0.20 compositions.

In order to see the picture more amicably, Inhibition of the grain growth due to the secondary phase formation on increasing Ho content is the cause for decreasing grain size [20].The relative intensity of the secondary phase in the present samples even after doping upto 20% is weak compared to the same ferrite of 5% dopant as reported earlier by other researchers [20], The particle size (t) was calculated using Debye-Scherrer formula. The average particle size decreases with increased in Holmium concentration. Table1 shows particle size, porosity parameter and density values. The densities of Ho doped Co ferrite were calculated by using Archimedes's principle. From density data it revealed that with increasing Ho Concentration in Co ferrite density goes on increasing. The lowest density shows value of 5.05 gm/cc for x=0.00 composition and x=0.20 shows highest value of density of 5.57 gm/cc. Percentage porosity values for x=0.00 to 0.20 series are lie in the order of 3.97 to 5.46%. For x=0.15 composition shows highest values of porosity and x=0.20 shows lowest value of porosity.

To get more convincing insight on the microscopic parameters pertaining to crystal structure room temperature neutron diffraction study was mooted on these samples. The cobalt ferrite samples being magnetic at room temperature, thus neutron diffraction study was able to give further evidence about the magnetic properties. The room temperature neutron diffraction data is also refined in the spinel structure in Fd-3m space group. The cell parameters, oxygen atom position, occupancies and site magnetic moment were put for refinement using starting

parameters for inverted spinel structure as described in the literature [22] and decent goodness of fitting parameters for crystal as well as magnetic part were obtained. The Rietveld refined room temperature neutron diffraction patterns are shown in fig 3 for $CoFe_{2-x}Ho_xO_4$ (x=0.0, 0.05, 0.10, 0.15 and 0.20) ferrites. The analysis of the data confirms the phase purity up to x = 0.10, we could identify the level of secondary phase ($HoFeO_3$) was up to 10-12% in x = 0.15 and 0.20 samples the impurity peak is marked by asterisk symbol (*). The additional peaks corresponding to magnetic ordering have been refined for magnetic structure for which, basis representation vector are determined by using *basireps* programme in *Fullprof* with the k vector (0 0 0) to correlate magnetic structure with crystal structure. The arrow in the fig 3 depicts the refined pattern with magnetic phase along with the crystal structure for all the samples.

Fig 4, summarizes the microscopic parameter determined from the neutron diffraction analysis. Fig 4 (a) shows the concentration dependent variation in the cell parameter, which show increase in the cell as Ho doping increase, this is expected because of large size of Ho ion. At highest doping concentration cell parameter remains more or less constant for highest percentage of Ho doping. It may be possible that the spinel lattice is compressed by the inter-granular secondary phase due to the differences in the thermal expansion coefficients [18]. Hence the increase of ‘‘a’’ with increasing concentration of Ho may suggest the existence of a solubility limit for Ho ions. Therefore, Ho introduction in $CoFe_2O_4$ affects not only the phase composition but also the size of the spinel matrix. While refining the Neutron diffraction data we fix Ho to occupy octahedral position, replacing Fe, but it is realized that best fitting of observed data is obtained when cation distribution is applied. Fig 4(b) and (c) shows the shows the cation distribution (Co and Fe) in the sample at tetrahedral and octahedral sites, which entail us that Fe concentration increases and Co concentration decrease at tetrahedral site, while at Octahedral site situation is reversed i.e. Fe concentration decreases and Co concentration increases. But overall we see that the (Fe-Co)-O bondlength increases uniformly for both at tetrahedral as well as octahedral site as depicted in fig 4 (d) and (e), possibly because of larger ionic radii of Ho ion. Correspondingly we also see that the magnetic moment as depicted in fig 4(f) also decreases with respect to increasing doping concentration, as Ho being non-magnetic at room temperature.

Morphology of the prepared Co–Ho nano-ferrites was observed from Scanning electron microscopy (SEM). Fig 5 shows SEM results. The results revealed that the grains are randomly shaped nanoparticles. It is also observed that with increase in Holmium content in cobalt ferrite,

porosity decreases. The agglomeration that has taken during the development of microstructure can be attributed to the strong magnetic nature of the samples. Similar is the behavior observed for are other rare earth doped Co ferrite [20]. For undoped cobalt ferrite the grains are square in shaped but once Ho is doped in cobalt ferrite its shows somewhat in spherical shape for Ho doped Co ferrite without secondary phase (x=0.05 and 0.10). For higher concentration of Ho in cobalt ferrite samples which contains secondary phase shows islands structure (x=0.15 and x=0.20).

Magnetization studies:

The M-H loops were measured at room temperature using a Vibrating Sample Magnetometer (VSM) for Ho doped $CoFe_2O_4$ powder samples at room temperature and the same are depicted in fig6. The magnetic parameters, including the saturation magnetization (Ms), coercive field (Hc), residual magnetization (Mr) have been extracted from the magnetization curves. Table 2 shows values of magnetization, coercivity and retentivity from VSM.The magnetic moment per formula unit expressed in Bohr magnetron (μ_B) is calculated by using the following relation, $\mu_{B=}$ M*Ms/5585, where M is the molecular weight of a particular ferrite composition and Ms is saturation magnetization(emu/gm). Un-doped cobalt ferrite shows higher magnetic moment but as Ho introduced in cobalt ferrite, value of magnetic moment goes on decreasing. For highest concentration of Ho in cobalt ferrite, the value of magnetic moment is lowest this is the case unlike studied earlier [25-27].The decrease in saturation, magnetization, coercivity and remanence can also be ascribed to weakening of AB-exchange interactions where A and B correspond to the element for the general formula of spinals given as AB_2O_4. The 4f electrons of rare earths (RE) like Ho^{3+} usually remain highly localized in the solid and form the magnetic electrons. This can be explained as a result of orbital screen effect. Therefore, the 4f electrons are screened from the crystal field by the 5d and 6s electrons. Hence cannot have strong magnetic interactions with neighboring cations. This leads to the decrease in the negative exchange interactions between Fe^{3+}–Fe^{3+}. Though the RE^{3+} –Fe^{3+} interaction (4f–3d coupling) and the RE^{3+}–RE^{3+} one (in direct 4f–5d–4f electrons coupling) exist but they are very weak.

In order to understand the effect of Ho doping on strain, magnetostriction study is carried out. Fig7 shows the magnetostriction curve for holmium doped cobalt ferrites measured at room temperature. From the fig7, variation of λ with magnetic field for Ho doped Co ferrite is

represented. It is seen that λ are negative in the magnetic field range of measurements, the maximum value of the strain, corresponding magnetic field and slope are summarized in table 3. It is evident from this table that for undoped cobalt ferrite i.e. x=0.0 composition shows highest magnetostriction value i.e. -202 ppm at 6500G. Further increase in Holmium content reduced the magnetostriction than x = 0.0. For x = 0.05 and x = 0.10, highest magnetostriction shows value of -196 ppm at 3500G and -119 ppm at 4000G respectively. For x=0.15 and x=0.20 with secondary phase shows magnetostriction values upto -98 ppm and -97 ppm both at 3000G respectively. Hence we can say that, the Ho doped Co ferrite with secondary phase shows reduction in magnetostrictive coefficient (λ). The slope of the magnetostriction curve is related to the stress sensitivity of the magnetization. Similar was the behavior obtained for other Ho doped ferrites [28-29]. The derivative of λ as a function of magnetic field (dλ/dH) is plotted as a function of magnetic fieldfor all samples i.e. x = 0.0 to x = 0.20 in fig 8. Fig clearly shows more prominent behavior in terms of dλ/dH for x = 0.05 cobalt ferrite, as holmium doping in cobalt ferrite increase, its slope (dλ/dH) increases. The decrease in the magnetostrictionon Ho doping and decrease in stress sensitivity for Ho concentration $x \geq 0.05$ clearly bring out the effect of doping. The x =0.05 composition has shown abnormal rise in stress sensitivity suggesting its suitability in magnetomechanical/Acoustic transducer. A small amount of Ho doping (x =0.05) causes exchange interaction between transition electrons and rare earth electrons. This is responsible for the abnormal rise in stress sensitivity for this particular composition. It is further perceived from fig 8 that the exchange interaction between the Rare earth ion and transition metal ion causes abnormal rise in stress sensitivity, while in other compositions the exchange interactions between transition- transitions metal ions (x= 0) and rare earth – rare earth metal ions seem to be dominant (x = 0.10, 0.15 and 0.20). This is also affirmed from the systematic decrease in magnetization as evinced from Hysteresis studies. Moreover, out of the three ordering R-R ion ordering is considered as the weakest one. This is reflected by marginal decrease in magnetostriction for x = 0.05 composition when compared to the undoped composition i.e. x = 0.0 and an appreciable decrease in magnetostrictionvalue for doping concentrations x = 0.15 and x = 0.20 (Table 3). It is also interesting to note that the two important parameters Retentivity and Coercivity are closely associated with magnetocrystalline anisotropy and there by associated with stress sensitivity. The initial rise and there after fall in

the values of residual magnetisation and Coercive field also upholds the abnormal behavior of x = 0.05 composition.

Conclusion:

We conclude that by optimizing our sol-gel based sample preparation technique we could produce Ho doped $CoFe_{2-x}Ho_xO_4$ phase pure spinel ferrite up to x=0.10 and neutron diffraction study revealed that the amount of secondary phase ($HoFeO_3$) for x=0.15 and x=0.20 is limited up to 10% which may be due to the solubility limit of Ho in the $CoFe_2O_4$ lattice. The Ho substitution in $CoFe_2O_4$ ferrite increases the lattice constantsand X-ray density. The analysis of the room temperature neutron diffraction study points out toward shortening of the bondlength further revealed that the magnetic moment decrease M-H loop were obtained from VSM, it shows there is a decrease in saturation magnetization, coercivity and retentivity because of anisotropic A-B site interactions. Undoped Co ferrite shows largest value of magnetostriction i.e.-202 ppm at 6500G. But an appreciable stress sensitivity especially in composition x =0.05 suggest useful applications in electronic devices.

Acknowledgement: The authors are grateful to UGC-DAE, Mumbai Centre for the financial support under CRS-M-203 to carry out this work. One of the authors D. M. Ghone acknowledges UGC-DAE, Mumbai Centre for providing the fellowship to carry out this work.

References:

[1] M. P. Horvath, Journal of Magnetism and Magnetic Materials 215 (2000) 171–183, B. Ramaswamy; S. D. Kulkarni, P. S. Villar, R. S. Smith, C. Eberly, R. C. Araneda, D. A. Depireux, Shapiro, Movement of magnetic nanoparticles in brain tissue: mechanisms and safety, Nanomedicine: Nanotechnology, Biology and Medicine 11, (2015), 1821–1829; IFT Conference Proceedings, Comprehensive Reviews in Food Science and Food Safety, 13,(2014).

[2] K. Maaz, S. Karim, A. Mashiatullah, J. Liu, M.D. Hou, Y.M. Sun, J.L. Duan, H.J. Yao, D. Mo, Y. F. Chen, Structural analysis of nickel doped cobalt ferrite nanoparticles prepared by co-precipitation route, Phys. B: Conden. Matter 404 (2009) 3947–3951.

[3] H. Wang, F. Zhang, W. Zhang, X. Wang, Z. Lu, Z. Qian, Y. Sui, D. Dong, W. Su, The effect of surface modification on the morphology and magnetic properties of $NiFe_2O_4$ nanoparticles, J. Cryst. Growth 293 (2006) 169–174.

[4] K. Maaz, S. Karim, A. Mumtaz, S.K. Hasnain, J. Liu, J.L. Duan, Synthesis and magnetic characterization of nickel ferrite nanoparticles prepared by co-precipitation route, J. Magn. Magn.Mater. 321 (2009) 1838–1842.

[5] Muhammad NaeemAshiq, Farah Naz, Muhammad AslamMalana, RuqiyaSehrishGohar, ZahoorAhmad,Role of Co–Cr substitution on the structural, electrical and magnetic properties of nickel nano-ferrites synthesized by the chemical co-precipitation method, Materials Research Bulletin 47 (2012) 683–686.

[6]WeimoZhu,LeiWang,RuiZhao,JiawenRen,GuanzhongLuandYanqinWang, Electromagnetic and microwave-absorbing properties of magnetic nickel ferrite nanocrystalsNanoscale, 3,(2011), 2862-2864.

[7]T. Ramesh, S. Senthil Kumar, R. S. Shinde and S. R. Murthy,Effect of aluminum substitution on structural and electromagnetic properties of nanocrystallineMgCuMn ferrites, AIP Conf. Proc. 1665, (2015), 130046.

[8]Hongyu Wang, Dongmei Zhu, Wancheng Zhou, Fa Luo, Synthesis and microwave absorbing properties of Ni–Cu ferrite/MWCNTs composites,Journal of Materials Science: Materials in Electronics,26, (2015) 7698–7704.

[9] M. Yehia , S. M. Ismail, A. Hashhash, Structural and Magnetic Studies of Rare-Earth Substituted Nickel Ferrites, Journal of Superconductivity and Novel Magnetism27,(2014), 771-774.

[10] Hemaunt Kumar, Jitendra Pal Singh, R. C. Srivastava, P. Negi, H. M. Agrawal and K. Asokan, FTIR and Electrical Study of Dysprosium Doped Cobalt Ferrite Nanoparticles, Journal of Nanoscience, 2014 (2014), 1-10.

[11] Erum Pervaiz and I H Gul, Influence of Rare Earth (Gd^{3+}) on Structural, Gigahertz Dielectric and Magnetic Studies of Cobalt ferrite, Journal of Physics: Conference Series 439, (2013), 012015.

[12] Jitendra Pal Singh, Hemanut Kumar, Ayush Singhal, Neelmanee Sarin, R. C. Srivastava and KeunHwaChae, Solubility limit, magnetic interaction and conduction mechanism in rare earth doped spinel ferrite, Appl. Sci. Lett. 2 (2016), 3-11.

[13] E. W. Lee, Magnetostriction and Magnetomechanical Effects, Rep. Prog. Phys., 18, (1955), 184-229.; R. Nongjai, S. Khan, K. Asokan, H. Ahmed and I. Khan, Impedance spectroscopic characterization of gadolinium substituted cobalt ferrite ceramics, J.Appl. Phys., 112, (2012), 084321; Y. Eom, M. Abbas, H. Noh and C. Kim, Morphology-controlled synthesis of highly crystalline Fe_3O_4 and $CoFe_2O_4$ nanoparticles using a facile thermal decomposition method, RSC Adv., 6 (2016),15861–15867.

[14] Rare Earth Materials: Properties and Applications by A.R. Jha, CRC Press, Taylor and Francis Group, (2014).

[15] Shyamsunder Goud, NakiraboinaVenkatesh, NamaHari Kumar, B. Rambabu,T. Somaiah, P. VeeraSomaiah, B. Ravinder Reddy, Synthesis and structural characterization of Sm doped Ni-Cd Nano Ferrites by Citrate-Gel Auto combustion method, Journal of Applied Chemistry, 8, (2015), 38-42.

[16] B.S. Randhawa' , H.S. Dosanjh, ManpreetKaur, Preparation of spinel ferrites from citrate precursor route—A comparative study, Ceramics International, 35, (2009), 1045–1049.

[17] Tokeer Ahmad and Irfan H. Lone, Citrate precursor synthesis and multifunctional properties of $YCrO_3$ nanoparticles, New J. Chem., 40, (2016),3216-3224.

[18]V. Siruguri, P. D. Babu, M. Gupta, A. V. Pimpale, and P. S. Goyal, Pramana J. Phys. 71 (2008)1197

[19] J. Rodriguez-Carvajal, *Physica B* 192, (1993), 55-69

[20] Irshad Ali, M.U. Islam, M. Ishaque, Hasan M. Khan, Muhammad Naeem Ashiq, M.U. Rana, Structural and magnetic properties of holmium substituted cobalt ferrites synthesized by chemical co-precipitation method, Journal of Magnetism and Magnetic Materials 324 (2012) 3773–3777.

[21] Sateesh Prathapani, M. Vinitha, T. V. Jayaraman, and D. Das, Effect of Er Doping on the Structural and Magnetic Properties of Cobalt-Ferrite, Journal of Applied Physics 115, (2014), 17A502-1-3

[22] S. J. Kim, B. R. Myoung, C. S. Kim, J. Appl. Phys. 93 (2003) 7504.

[23] Jiang Jing, Li Liangchao, XuFeng, Structural Analysis and Magnetic Properties of Gd-Doped Li-Ni Ferrites Prepared Using Rheological Phase Reaction Method Journal of Rare Earths, 25, (2007), 79-83

[24] S. G. Kakade, R. C. Kambale, C. V. Ramanna, Y. D. Kolekar, Crystal strain, chemical bonding, magnetic and magnetostrictive properties of erbium (Er^{3+}) ion substituted cobalt-rich ferrite ($Co_{1.1}Fe_{1.9-x}Er_xO_4$), RSC Adv.6 (2016), 33308-33317

[25] Sheena Xavier, SmithaThankachan, Binu P. Jacob, E.M. Mohammed, Effect of Sintering Temperature On The Structural And Magnetic Properties of Cobalt Ferrite Nanoparticles, Nanosystems: Physics, Chemistry, Mathematics, 4 (2013), 430–437.

[26] Jiang Jing, Li Liangchaosky, XuFeng, Structural Analysis and Magnetic Properties of Gd-Doped Li-Ni Ferrites Prepared Using Rheological Phase Reaction Method,Journal of Rare Earths, 25, (2007), 79-83.

[27] A. A. Kadam, S. S. Shinde, S. P. Yadav, P. S. Patil, K.Y. Rajpure, Structural, morphological, electrical and magnetic properties of Dy doped Ni–Co substitutional spinel ferrite, Journal of Magnetism and Magnetic Materials, 329,(2013), 59–64.

[28] Panneer Muthuselvam, R.N. Bhowmik, Mechanical alloyed Ho^{3+} doping in $CoFe_2O_4$ spinel ferrite and understanding of magnetic nanodomains, Journal of Magnetism and Magnetic Materials, (2010), 767–776.

[29] K. Kamala Bharathi, G. Markandeyulu, and C. V. Ramana, Structural, Magnetic, Electrical, and Magnetoelectric Properties of Sm- and Ho-Substituted Nickel Ferrites, J. Phys. Chem.,115(2011),554–560.

Figure captions

Fig 1: (color online) Pictorial representation of reaction mechanism in sol-gel combustion route

Fig 2: (color online) X-ray diffractograms of $CoFe_{2-x}Ho_xO_4$ ferrites (x=0.0, 0.05, 0.10, 0.15, 0.20). Open symbol represents the observed data, red line is calculated data, blue line represents the difference between observed and calculated pattern while green ticks represents the Brags peaks.

Fig 3: (color online) Neutron diffraction of $CoFe_{2-x}Ho_xO_4$ ferrites (x=0.0, 0.05, 0.10, 0.15, 0.20) at room temperature. Open symbol represents the observed data, red line is calculated data, blue line represents the difference between observed and calculated pattern while green ticks represents the Brags peaks. The arrow mark shows the magnetic peak while asterisk mark shows peak corresponding to secondary $HoFeO_3$ phase.

Fig 4: (color online) Microscopic parameters of $CoFe_{2-x}Ho_xO_4$ ferrites (x=0.0, 0.05, 0.10, 0.15, 0.20) determined from the analysis of neutron diffraction. Fig 4(a) represents lattice constants with doping concentration. Fig 4(b) and (c) are corresponds to Fe-Co concentration at tetrahedral and octahedral sites. Fig 4 (d) and (e) shows variation of the (Fe-Co)-O bondlength corresponds to tetraheadral and octahedral site with respect to concentration variation. Fig 4 (f) shows magnetic moment variation with respect to concentration.

Fig 5: (color online) SEM images for $CoFe_{2-x}Ho_xO_4$ ferrites (x=0.0, 0.05, 0.10, 0.15, 0.20)

Fig 6: (color online) Magnetization study for $CoFe_{2-x}Ho_xO_4$(x=0.0, 0.05, 0.10, 0.15, 0.20) ferrite.

Fig 7: (color online) Magnetostriction results for $CoFe_{2-x}Ho_xO_4$(x=0.0, 0.05, 0.10, 0.15, 0.20) ferrite.

Fig 8: (color online) Derivative of magnetostriction as a function of field for $CoFe_{2-x}Ho_xO_4$(x=0.0, 0.05, 0.10, 0.15, 0.20)ferrite

Fig 1:

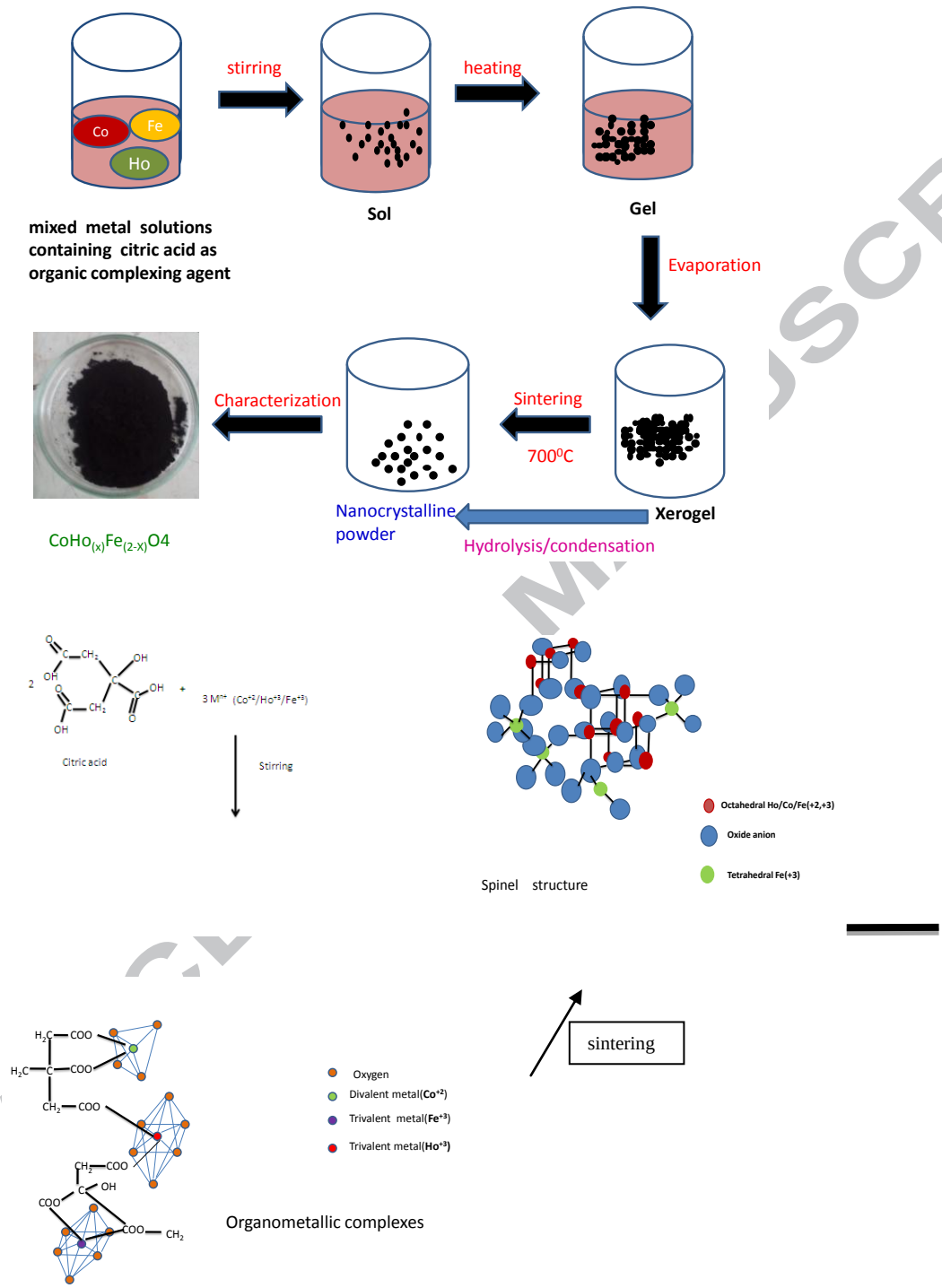

Fig 2:

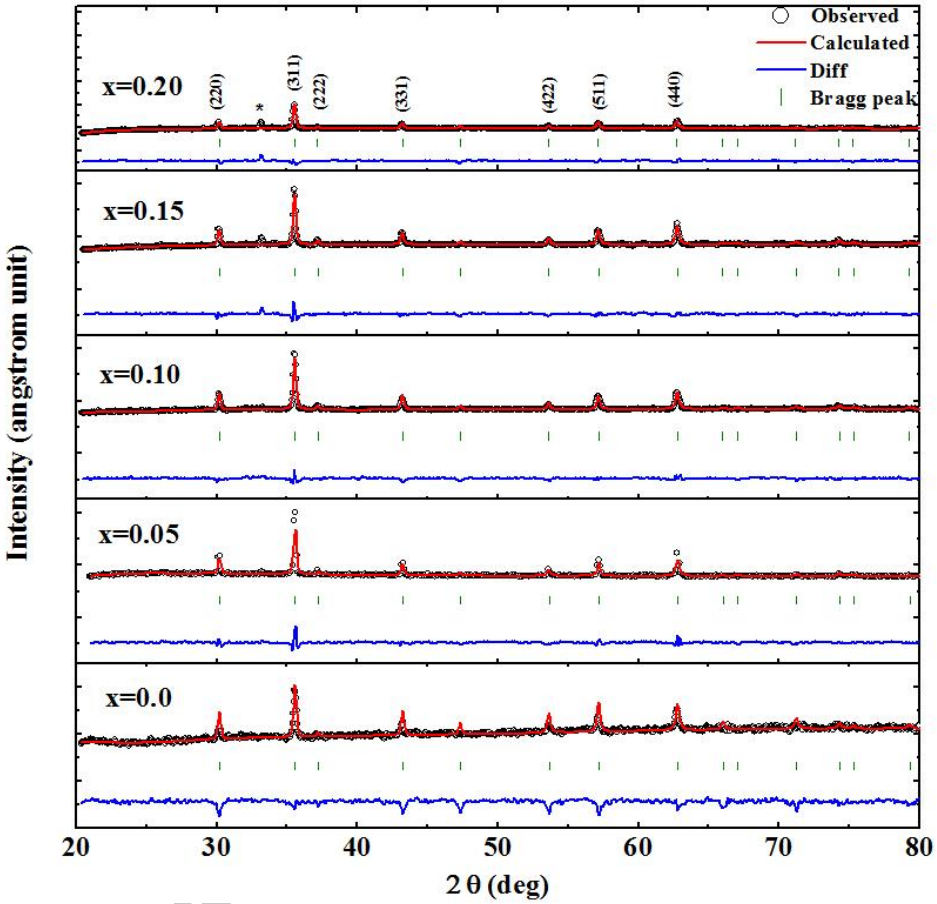

Fig 3:

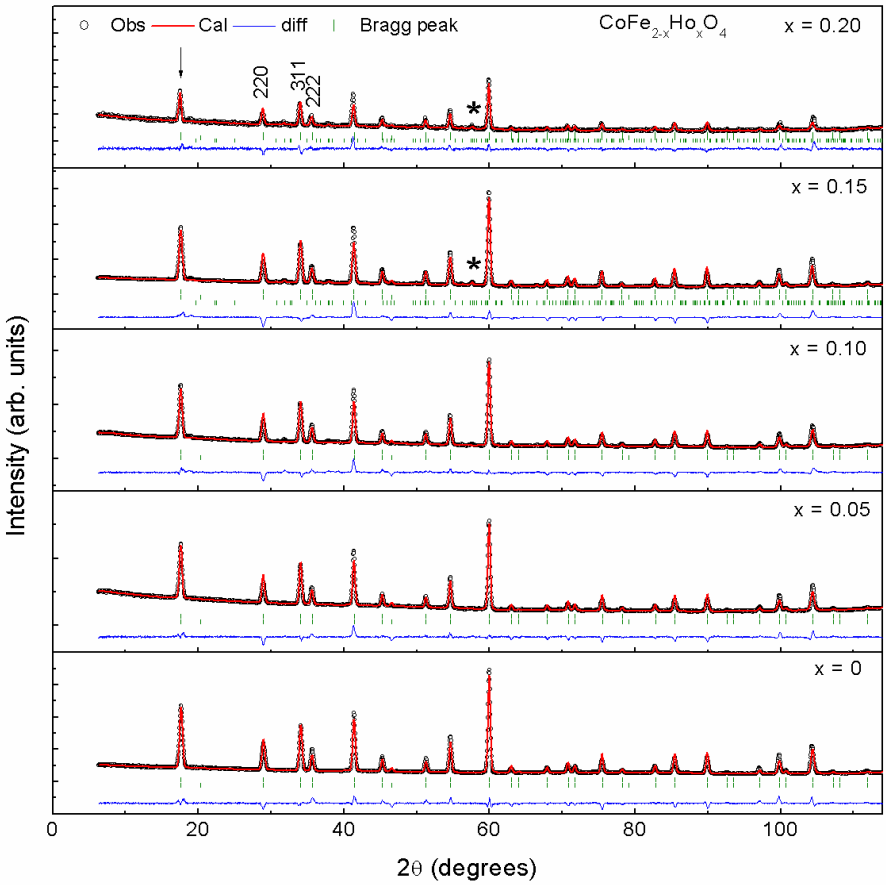
Obs
Cal
diff
Bragg peak
CoFe2-xHoxO4
x = 0.20
220
311
222
*
x = 0.15
*
x = 0.10
x = 0.05
x = 0
Intensity (arb. units)
0
20
40
60
80
100
2θ (degrees)

Fig 4:

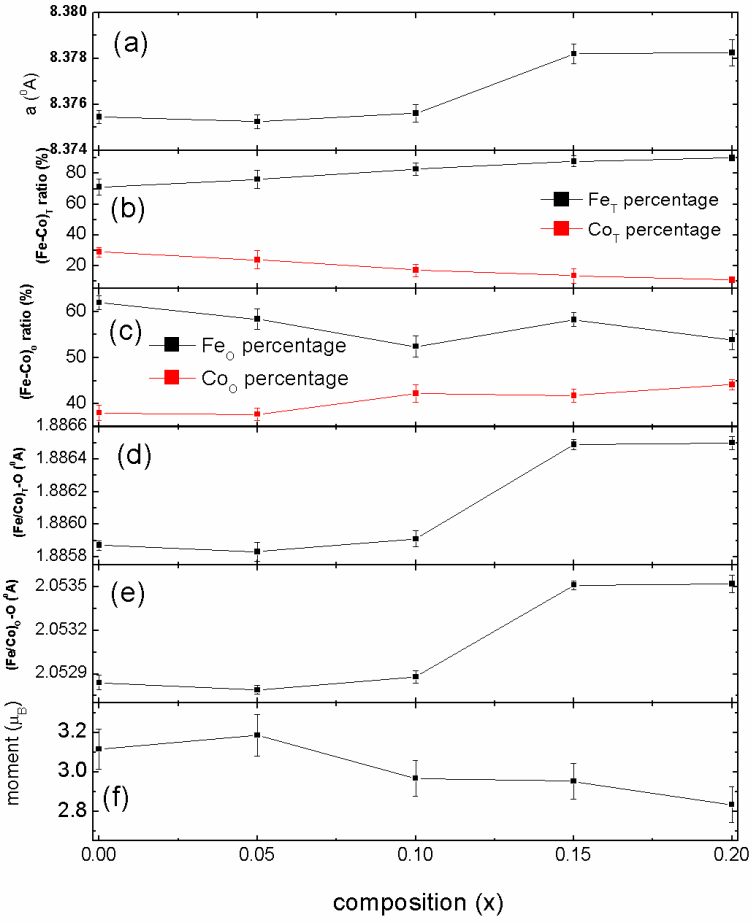
(a)
a (Å)
8.380
8.378
8.376
8.374
(b)
(Fe-Co)T ratio (%)
80
60
40
20
FeT percentage
CoT percentage
(c)
(Fe-Co)O ratio (%)
60
50
40
FeO percentage
CoO percentage
(d)
(Fe/Co)T-O (Å)
1.8866
1.8864
1.8862
1.8860
1.8858
(e)
(Fe/Co)O-O (Å)
2.0535
2.0532
2.0529
moment (μB)
(f)
3.2
3.0
2.8
0.00
0.05
0.10
0.15
0.20
composition (x)

Fig 5:

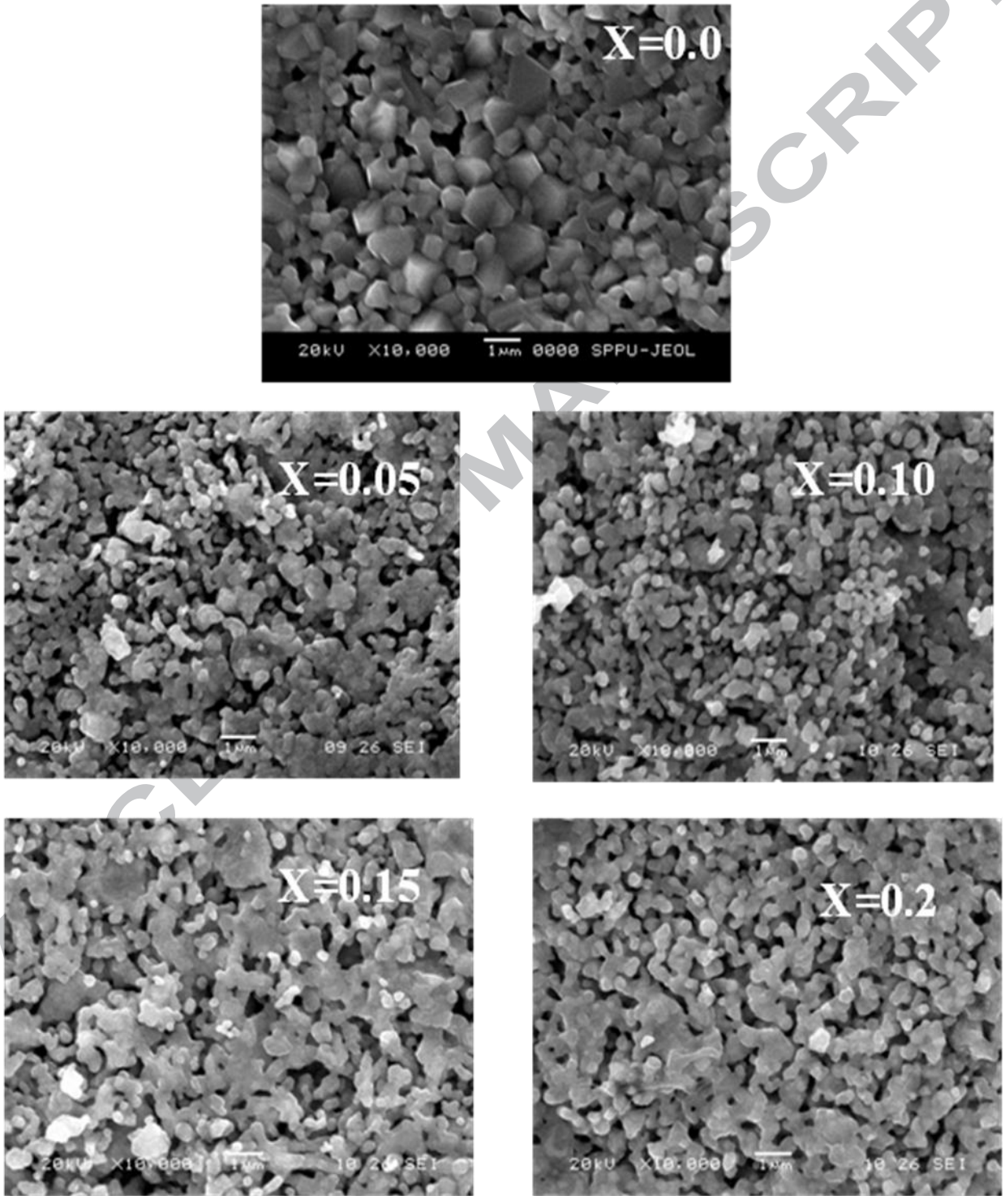

Fig 6:

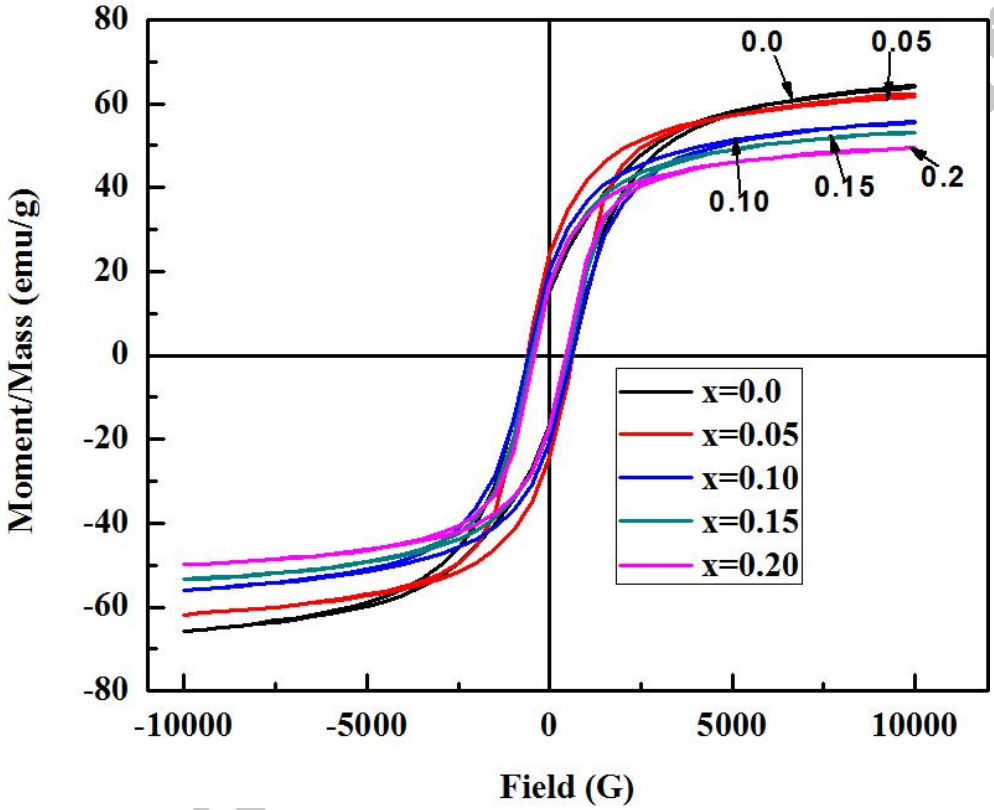

Fig 7:

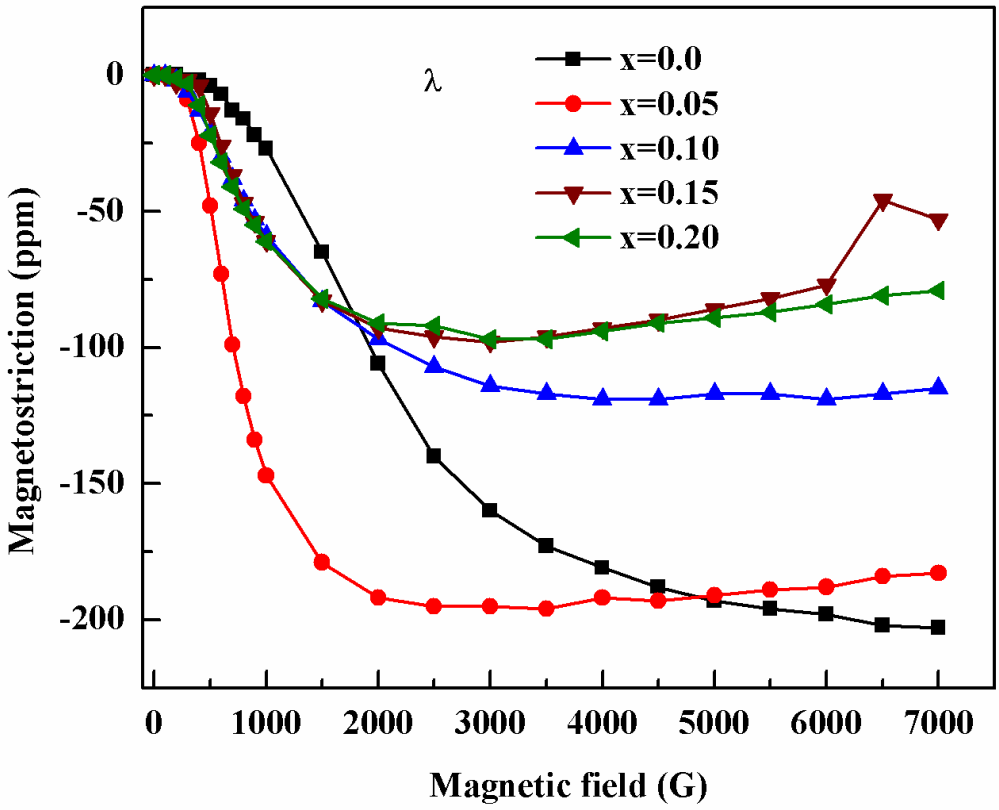

Fig 8:

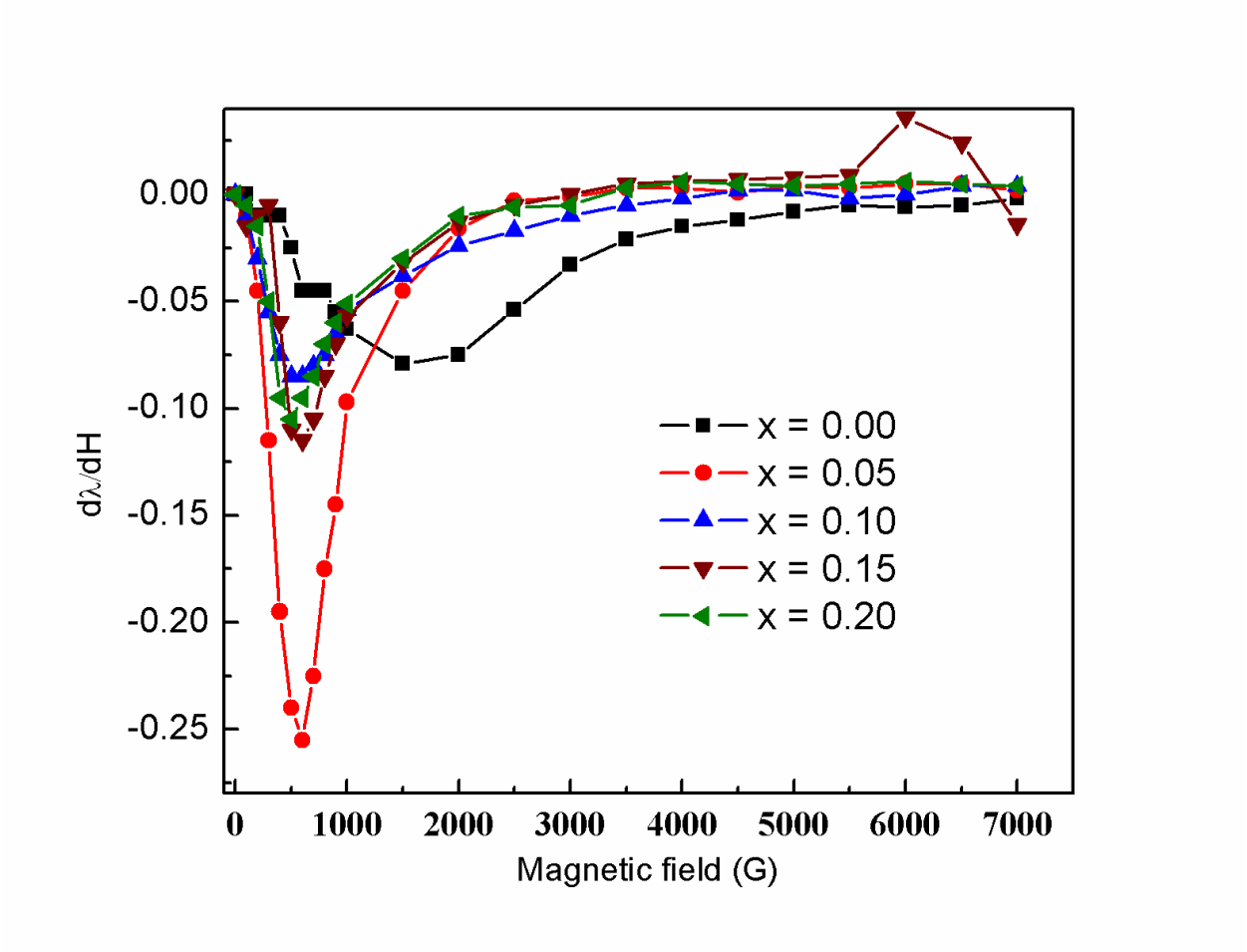

Table1. ***Structural parameters*** **for $CoFe_{2-x}Ho_xO_4$**

Sr. No	Samples Name	Crystallite size (nm)	Theoretical density (gm/cm^3)	Calculated density (gm/cm^3)	Porosity (%)
1.	x=0.00	64.39	5.31	5.05	4.89
2.	x=0.05	75.81	5.44	5.15	5.34
3.	x=0.10	75.79	5.56	5.30	4.68
4.	x=0.15	75.77	5.68	5.37	5.46
5.	x=0.20	72.68	5.80	5.57	3.97

Table2: magnetic parameters for $CoFe_{2-x}Ho_xO_4$.

Sample	Magnetization emu/g	Coercivity G	Retentivity emu/g	Magnetic moment (Bohr magnetron)
x=0.00	65.02	591.83	16.049	2.72
x=0.05	61.961	618.80	24.144	2.65
x=0.10	55.805	594.61	20.492	2.44
x=0.15	53.312	508.37	17.614	2.39
x=0.20	49.748	440.70	17.033	2.28

Table 3: Magnetostriction values for $CoFe_{2-x}Ho_xO_4$.

Sr.No	Sample	Magnetostriction (ppm)	dλ/ dH (ppm/G)	Field for maximum magnetostriction
1.	x=0.00	-202	0.04	6500
2.	x=0.05	-196	0.06	3500
3.	x=0.10	-119	0.05	4000
4.	x=0.15	-98	0.04	3000
5.	x=0.20	-97	0.04	3000

Highlights of our manuscript (MGMA_2017_3157) titled "**Structural and physical property study of sol – gel synthesized $CoFe_{2-x}Ho_xO_4$ nano ferrites"**

* Ho doped CoFe2O4 sample are prepared using modified Sol-gel technique.

* Room temperature Neutron diffraction study shows phase purity in the sample preparation.

* The single phase doping concentration of Ho up to 10% is achieved in CoFe2O4 at Fe site.

* Magnetostriction study in 5* Ho doped $CoFe_2O_4$ compound shows interesting behavior.